2021

A Method of Mapping Heat Exchanger as Simple Polynomials

Deokgeun Park
Texas A&M University, United States of America, dpark18@tamu.edu

Fangzhou Guo

Bryan P. Rasmussen

A Method of Mapping Heat Exchanger as Simple Polynomials

Deokgeun Park[1], Fangzhou Guo[1], Bryan Rasmussen[1]

[1]Texas A&M University, J. Mike Walker '66 Department of Mechanical Engineering,
College Station, TX, USA
dpark18@tamu.edu

ABSTRACT

Conducting economic comparison studies of vapor-compression systems early in the product development process allows the designer to balance competing objectives of raw material costs, life-cycle cost, and system performance. However, detailed performance simulation models typically require iterative solutions at both the component and system levels. These nested iterative models make economic comparison studies computationally prohibitive. To address the challenge of nested iterations, non-iterative polynomial representations of components can be implemented. In this paper, a method to represent the heat exchangers' effectiveness, pressure loss, refrigerant charge, and mass with non-iterative models is presented. A method of mapping the heat exchanger using Monte Carlo sampling over its operational and design space is given. The method is then applied to map the heat exchanger effectiveness, refrigerant charge level, pressure drop, and mass of a flooded type shell and tube heat exchanger. Heat exchangers are represented as a function of inlet conditions and heat exchanger geometries. This proposed method of representing heat exchanger as a polynomial map relieves the computationally heavy nature of finite control volume modeling of heat exchangers with non-iterative empirical maps. Such a method of mapping heat exchangers enables rapid iterations of the system model, thus enabling effective economic trade-off studies of vapor-compression systems.

1. INTRODUCTION

Chiller manufacturers face the emergence of new and different regulations around the globe and changes in customer demands. In the development of a chiller system, components are put together to meet the system level requirements such as cooling capacity and system efficiency. However, many chiller configurations are possible in meeting such requirements. The difficulty lies in deciding which configuration is better than others. For example, different types of compressors can be used in a chiller. To evaluate the advantages and disadvantages of using a particular compressor as opposed to another, there needs to be a way to compare different system configurations.

One way to evaluate the cost-effectiveness of a compressor is to let the design of the heat exchanger to be iteratively solved to meet the system requirements. The effect of the compressor has on the raw material cost of the heat exchangers needed to meet the cooling capacity, and the efficiency could be used to evaluate the impact of the compressor in a chiller system. The flowchart in Figure 1 shows an example of an algorithm used to solve a chiller model. The component models for the evaporator and the condenser, just like the system model, require iterations to converge to a solution. The consequence of this is "nested iterations" for the system level convergence. The nested iterations required for the system-level convergence cause an increase in computational time. However, with the implementation of non-iterative component models, the system-level convergence process gets simplified, as shown in Figure 2.

For the system to converge without nested iterations, non-iterative maps representing the heat exchanger effectiveness, pressure loss, refrigerant charge, and mass as a function of inlet conditions and heat exchanger design variables are needed. In this paper, a method of empirically mapping heat exchangers will be developed to solve steady state conditions for different chiller configurations quickly. Evaluation of economic viability and comparison between different chiller configurations over a wide range of test conditions will be enabled by the simple polynomial mapping of heat exchangers.

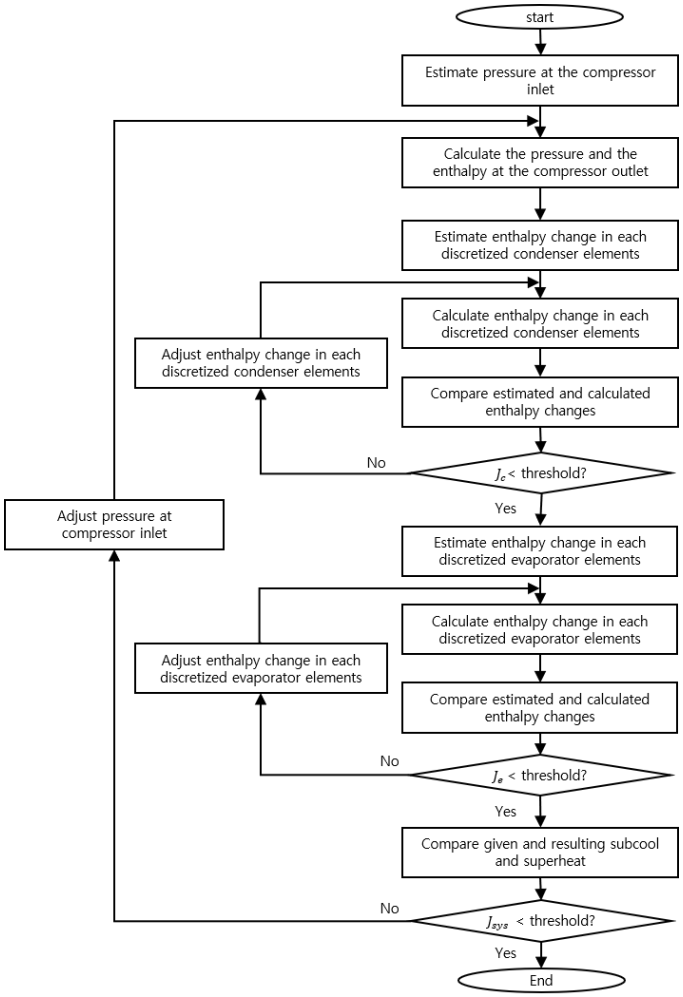

Figure 1: Flowchart of chiller solving algorithm with nested iterations

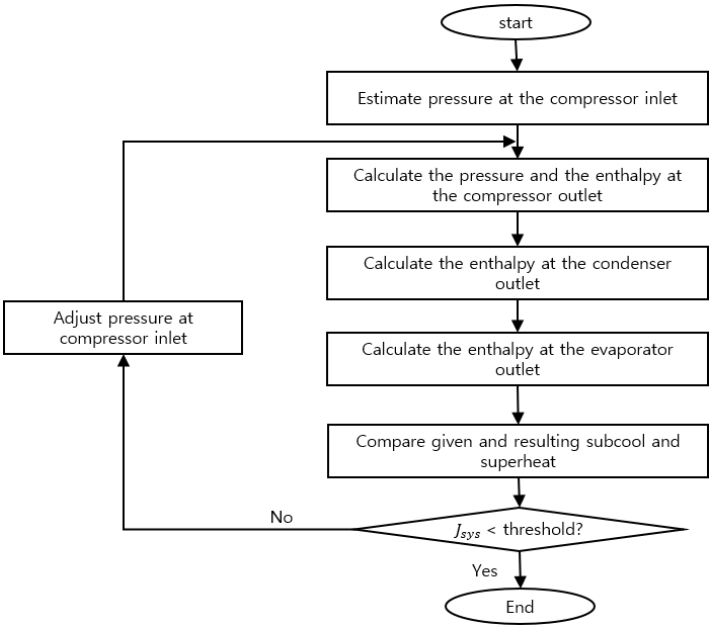

Figure 2: Flowchart of chiller solving algorithm with non-iterative heat exchanger models

2. LITERATURE REVIEW

In this section, a review of common modeling methods for steady state performance of compressors and heat exchangers will be conducted. Modeling of chiller components can be categorized into physics-based models and empirical map-based models. Physics-based modeling predicts the outlet conditions by simulating the physical mechanisms inside of the component. Detailed information about the component's geometry and physical properties is needed to create a physics-based model. In comparison, the map-based approach bypasses the detailed physics of the component and seeks to generate a mapping function that directly relates the inlet conditions to the outlet conditions. As previously mentioned in the Introduction section, iterative component models cause nested iterations and a significant increase in computational time. Therefore, this paper will focus on the use of non-iterative map-based component modeling for its simplicity and superiority in computational speed. Other advantages of map-based modeling include the direct use of inlet and outlet conditions to generate the map, which avoids model calibration.

For heat exchangers, artificial neural network (ANN) can be used for empirical modeling. Various types of condensers, liquid line suction heat exchangers and evaporators, run-around heat exchangers, compact heat exchangers, plate type heat exchangers, fin and tube heat exchangers, solar energy collectors, shell and tube heat exchangers, direct contact type heat exchanger, earth to air heat exchangers, heat exchangers used in power plants and special purpose heat exchangers are modeled using ANN in the literature (Mohanraj *et al.*, 2015). ANN mimics the way the biological system processes information. Hidden layers are placed in between the input and output layers, which are provided. Neurons are set inside the hidden layers, and the weights are optimized to fit the given data. Then, an optimized ANN model can be used to make predictions. In the case of the shell and tube heat exchanger, ANN models are used by Mandavgane and Pandharipande (2006), Pandharipande *et al.* (2004), and Jasim (2013) to predict cold and hot outlet temperatures. Studies by Xie *et al.* (2007) and Wang *et al.* (2006) modeled heat transfer rate, and El-Said *et al.* (2021) modeled pressure drop in the heat exchanger, along with outlet temperature predictions. Hojjat (2020) modeled Nusselt number and pressure drop, and Iyengar (2015) modeled the overall heat transfer and pressure drop. Ahilan *et al.* (2011b) predicted overall heat transfer using ANN. The fouling coefficient of the heat exchangers was modeled by Navvab Kashani *et al.* (2012) and Ahilan *et al.* (2011a).

Some of the shortcomings of ANN include overfitting and the need to optimize the network parameters. Overfitting can occur when there is over-training with too many iterations (Yin *et al.*, 2003). In order to prevent over-training of ANN, error backpropagation and Levenberg-Marquardt algorithms for over-training resilience (EBaLM-OTR) technique are proposed (Wijayasekara *et al.*, 2011). Learning rate, number of hidden layers, and number of neurons in the hidden layers are a few examples of the network parameters that need to be optimized. Choosing the number of neurons in the hidden layer is a trial and error process (Gang and Wang, 2013). There is no formula for the optimal number of neurons in the hidden layers, which is still an active area of research. In order to relieve the need for optimization associated with ANN, an alternative and universal empirical mapping method for the heat exchanger is needed.

3. HEAT EXCHANGER MODELING

A discretized heat exchanger element is shown in Figure 3. For each element, refrigerant enthalpy, pressure and mass flowrate at the inlet are given. Secondary fluid inlet temperature and mass flow rate are given as well. Assuming steady-state conditions, temperature of the heat exchanger wall will remain constant and Equation (1) shows the heat transfer rate from the refrigerant to the heat exchanger wall equaling the heat transfer rate from the heat exchanger wall to the secondary fluid. Using heat transfer coefficient from the literature, given fluid temperatures at the inlet and the heat exchanger geometry, the heat exchanger wall temperature can be solved using Equation (2) and Equation (3). Then, heat transfer rate from the refrigerant to the heat exchanger wall can be back calculated and the enthalpy of the refrigerant at the outlet can be calculated using Equation (4).

$$\dot{Q}_i = \dot{Q}_o = \dot{Q}_r \tag{1}$$

$$\dot{Q}_i = \alpha_i A_i (T_r - T_w) \tag{2}$$

$$\dot{Q}_o = \alpha_o A_o (T_w - T_o) \tag{3}$$

$$\dot{Q}_r = \dot{m}_o h_o - \dot{m}_i h_i \tag{4}$$

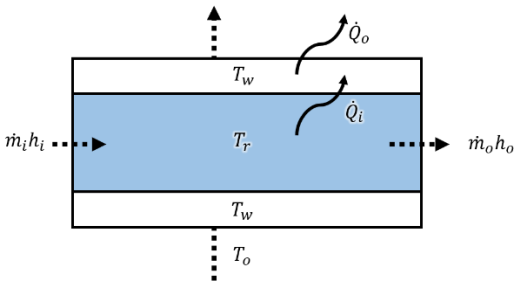

Figure 3: A discretized heat exchanger element

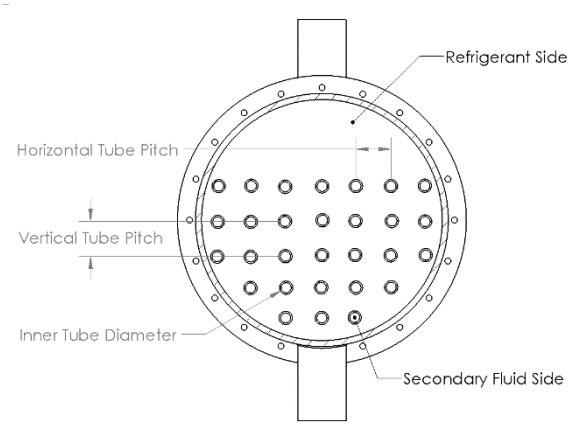

Figure 4: Single pass flooded shell and tube type heat exchanger cross-section

Using finite control volume modeling method, this paper will develop a universal mapping method for heat exchangers. Brazed plate, microchannel, plate-fin, tube in tube, shell and tube flood type, and shell and tube direct expansion type heat exchangers were successfully modeled with this method. However, only a shell and tube flooded-type heat exchanger will be presented in this paper to avoid redundancy. Figure 4 shows a CAD drawing of a flooded shell and tube heat exchanger. The universal mapping method can be applied to a wide range of heat exchangers with different geometries, including the flooded-type shell and tube heat exchanger.

3.1 Shell-side Heat Transfer Correlation

A flooded type shell and tube heat exchanger (STFL) evaporator was chosen for its wide application in the industry. The STFL heat transfer coefficients for two-phase boiling were referenced from Hwang and Yao (1986). Shell side heat transfer coefficient (α_o) is expressed as a general form of correlation from Chen (1966).

$$\alpha_o = S\bar{\alpha}_{nb} + F\alpha_l \tag{5}$$

Where $S, \bar{\alpha}_{nb}, F, \alpha_l$ are suppression factor, average nucleate boiling heat transfer coefficient, two-phase Reynolds number factor and liquid-only forced convective heat transfer coefficient, respectively. Single-phase heat transfer coefficients for the STFL were modeled using the Churchill and Bernstein (1977) method. For the intermediate regime, where $Re < 10000$, the following correlation for the average Nusselt number is used.

$$\overline{Nu} = 0.3 + \frac{0.62 Re^{\frac{1}{2}} Pr^{\frac{1}{3}}}{\left[1 + (0.4/Pr)^{\frac{2}{3}}\right]^{\frac{1}{4}}} \tag{6}$$

For $10000 < Re < 40000$, the following average Nusselt number is used.

$$\overline{Nu} = 0.3 + \frac{0.62Re^{\frac{1}{2}}Pr^{\frac{1}{3}}}{\left[1+(0.4/Pr)^{\frac{2}{3}}\right]^{\frac{1}{4}}}\left[1+\left(\frac{Re}{282000}\right)^{\frac{5}{8}}\right]^{\frac{4}{5}} \quad (7)$$

For $40000 < Re < 400000$, the average Nusselt number is shown below.

$$\overline{Nu} = 0.3 + \frac{0.62Re^{\frac{1}{2}}Pr^{\frac{1}{3}}}{\left[1+(0.4/Pr)^{\frac{2}{3}}\right]^{\frac{1}{4}}}\left[1+\left(\frac{Re}{282000}\right)^{\frac{1}{2}}\right] \quad (8)$$

3.2 Tube-side Heat Transfer Correlation

Tube-side heat transfer coefficients are referenced from Gnielinski (1975). For $2400 < Re$, the following Nusselt number is used.

$$\overline{Nu} = \frac{\frac{f}{8}(Re-100)Pr}{1+12.7\left(\frac{f}{8}\right)^{0.5}\left(Pr^{\frac{2}{3}}-1\right)} \quad (9)$$

For $Re < 2400$, the following Nusselt number is used.

$$\overline{Nu} = 4.364 \quad (10)$$

3.3 Heat Exchanger Solving Method

After the heat exchanger model is established and discretized, an optimizer is used to solve the heat exchanger iteratively. u_{ext} and u_{ini} are inputs to the optimizer. As shown in Equation (11), u_{ext} is a vector of external conditions such as enthalpy of the refrigerant at the inlet (h_{ri}) and temperature of secondary fluid at the inlet (T_{si}). u_{ini} is defined in Equation (12). Vector of enthalpy change in each heat exchanger elements ($\overline{\Delta h}_r$) is iteratively solved by the optimizer to minimize the value of the objective function.

$$u_{ext} = \begin{bmatrix} h_{ri} \\ T_{si} \end{bmatrix} \quad (11)$$

$$u_{ini} = \left[\overline{\Delta h}_r\right] \quad (12)$$

Equation (13)-(15) defines transformation matrix R that maps working fluid elemental enthalpy change (u_{ini}) to a vector of elemental working fluid enthalpy changes ($\overline{\Delta h}_r$) and secondary fluid temperature change ($\overline{\Delta T}_s$). r is defined as the refrigerant mass flow rate ($\dot{m}_r$) divided by external fluid mass flow rate ($\dot{m}_{ext}$) and heat capacity (C_{ext}).

$$\begin{bmatrix} \overline{\Delta h}_r \\ \overline{\Delta T}_s \end{bmatrix} = R u_{ini} \quad (13)$$

$$R = \begin{bmatrix} 1 & 0 & 0 \\ 0 & \ddots & 0 \\ 0 & 0 & 1 \\ \hline r & 0 & 0 \\ 0 & \ddots & 0 \\ 0 & 0 & r \end{bmatrix} \quad (14)$$

$$r = -\frac{\dot{m}_r}{\dot{m}_{ext} C_{ext}} \tag{15}$$

Ru_{ini} added to u_{ext} yields a vector of outlet enthalpies of the refrigerant and the secondary fluid out of the elements, as shown in Equation (16). In Equation (17), N and M are transformation matrices that depend on the geometric nature of each heat exchanger type. N and M transform the optimizer inputs, u_{ini} and u_{ext}, into the enthalpy and temperature inputs to the element-wise solver, respectively.

$$\begin{bmatrix} \bar{h}_{ro} \\ \bar{T}_{so} \end{bmatrix} = \begin{bmatrix} \overline{\Delta h}_r \\ \overline{\Delta T}_s \end{bmatrix} + \begin{bmatrix} \bar{h}_{ri} \\ \bar{T}_{si} \end{bmatrix} \tag{16}$$

$$\begin{bmatrix} \bar{h}_{ri} \\ \bar{T}_{si} \end{bmatrix} = \left(\begin{bmatrix} N_1 & 0 \\ 0 & M_1 \end{bmatrix} \begin{bmatrix} \bar{h}_{ro} \\ \bar{T}_{so} \end{bmatrix} + \begin{bmatrix} N_2 & 0 \\ 0 & M_2 \end{bmatrix} u_{ext} \right) \tag{17}$$

From the optimizer inputs (u_{ini}), input vector to the element-wise solver (u_{eli}) is determined. With u_{eli}, the element-wise solver computes the enthalpy and temperature at the outlet. Equation (18)-(20) shows this process.

$$u_{eli} = \begin{bmatrix} \bar{h}_{ri} \\ \bar{T}_{si} \end{bmatrix} \tag{18}$$

$$u_{eli} = \left(\begin{bmatrix} I - N_1 & 0 \\ 0 & I - M_1 \end{bmatrix}^{-1} \right) * \left(\begin{bmatrix} N_1 & 0 \\ 0 & M_1 \end{bmatrix} Ru_{ini} + \begin{bmatrix} N_2 & 0 \\ 0 & M_2 \end{bmatrix} u_{ext} \right) \tag{19}$$

$$u_{elo} = \begin{bmatrix} \bar{h}_{ro} \\ \bar{T}_{so} \end{bmatrix} \tag{20}$$

For simplicity, parts of Equation (12) are redefined with expressions from Equation (21)-(23).

$$K = \begin{bmatrix} I - N_1 & 0 \\ 0 & I - M_1 \end{bmatrix}^{-1} \tag{21}$$

$$NM_1 = \begin{bmatrix} N_1 & 0 \\ 0 & M_1 \end{bmatrix} \tag{22}$$

$$NM_2 = \begin{bmatrix} N_2 & 0 \\ 0 & M_2 \end{bmatrix} \tag{23}$$

Shown in Equation (24) and (25), J is the objective function and u_{re} is the elemental solver residual, which is the difference between the input vector to the elemental solver u_{eli} and output vector from the elemental solver u_{elo}.

$$u_{re} = u_{elo} - u_{eli} \tag{24}$$

$$J = \left\| \frac{u_{re} - u_{ini}}{u_{re}} \right\|_2 \tag{25}$$

The optimizer iterates on this process until the objective function is sufficiently small and satisfies the stopping criterion. As the iteration halts, the resulting refrigerant charge and heat exchanger mass information are stored together, along with the capacity of the heat exchanger.

3.4 Monte Carlo Sampling

Monte Carlo simulation utilizes randomness in its sampling method to survey potential outcomes of its decision space. For a heat exchanger, a given range of mass flow rates, pressures, inlet quality, and heat exchanger design variables are explored with the Monte Carlo sampling method.

3.5 Heat Exchanger Mapping Method

With a finite set of test points from the Monte Carlo sampling of the operation and design spaces, a map of the heat exchanger is ready to be created. Effectiveness, refrigerant charge, pressure drop, and mass are mapped as a function of pressure (P_{in}), refrigerant mass flow rate ($\dot{m}_r$), inlet quality (x_{in}), secondary fluid inlet temperature (T_{si}) and design variables (L). The effectiveness of the heat exchanger is defined in Equation (26).

$$\varepsilon = \frac{\dot{Q}_{hx}}{C_s \cdot \dot{m}_r \cdot (T_r - T_s)} \tag{26}$$

$$\begin{aligned}\{\varepsilon, m_{ch}, \Delta P_{hx}, m_{hx}\} = {} & d_1 + d_2 L + d_3 T_{si} + d_4 P_{in} + d_5 \dot{m}_r + d_6 x_{in} + d_7 L^2 + d_8 L T_{si} + d_9 L P_{in} + \\ & d_{10} L \dot{m}_r + d_{11} L x_{in} + d_{12} {T_{si}}^2 + d_{13} T_{si} P_{in} + d_{14} T_{si} \dot{m}_r + d_{15} T_{si} x_{in} + d_{16} {P_{in}}^2 + d_{17} P_{in} \dot{m}_r + \\ & d_{18} P_{in} x_{in} + d_{19} {\dot{m}_r}^2 + d_{20} \dot{m}_r x_{in} + d_{21} {x_{in}}^2\end{aligned} \tag{27}$$

Equation (27) shows mapping equation for effectiveness, charge, pressure drop and heat exchanger mass. Although only the length of flooded type shell and tube heat exchanger was chosen as the design variable for simplicity, the expendable nature of the map allows multiple design variables to be used, if desired.

4. RESULTS AND DISCUSSION

Comparison between the sampled data and mapped predictions are presented for a flooded type shell and tube condenser. As shown in Figure 5, heat exchanger effectiveness, refrigerant charge level, and mass show an excellent prediction using the polynomial mapping approach.

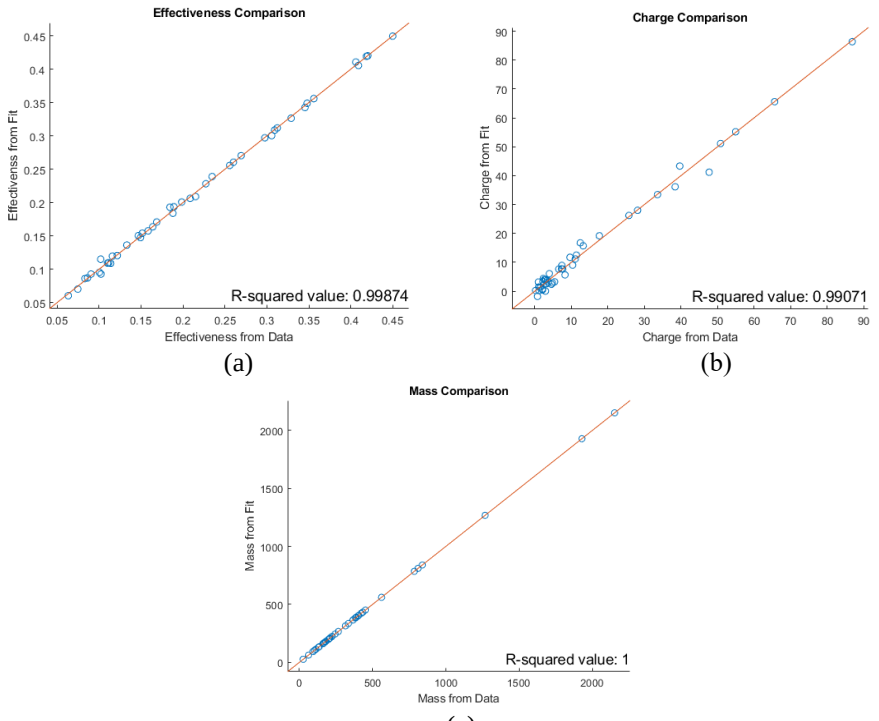

Figure 5: Heat exchanger effectiveness (a), refrigerant charge level (b), and mass (c) comparison

The map of heat exchanger pressure loss is not generated since the STFL is assumed to have negligible pressure loss.

5. CONCLUSIONS

A method, universal to all types of heat exchangers, of mapping heat exchanger's effectiveness, refrigerant charge level, mass, and pressure drop as simple polynomials was explored. The comparison of the prediction and polynomial map shows excellent prediction. Simple polynomials can represent a heat exchanger in the system level solver, eliminating the nested loops and the computationally heavy nature of the finite control volume modeling. Furthermore, the mapping method using polynomials is scalable to the full design variable set, enabling fast multi-objective system-level optimization of vapor compression systems.

NOMENCLATURE

A	Area	$(m\text{^}2)$
C	Heat capacity	$(J/\,℃)$
d	Heat exchanger mapping coefficients	$(-)$
f	Frictional loss	$(-)$
F	Two-phase Reynolds number factor	$(-)$
h	Enthalpy	(kJ/kg)
J	Objective function	$(-$
K	Simplification matrix	$(-)$
L	Heat exchanger length	(m)
M	Temperature transformation matrix	$(-)$
m	Mass	(kg)
$\dot{m}$	Mass flow rate	(kg/s)
N	Enthalpy transformation matrix	$(-)$
NM	Simplification Matrix	$(-)$
Nu	Nusselt number	$(-)$
$\overline{Nu}$	Average Nusselt number	$(-)$
P	Pressure	(Pa)
Pr	Prandtl number	$(-)$
$\dot{Q}$	Capacity	(kW)
r	Elemental transformation matrix element	$(℃/J)$
R	Elemental transformation matrix	$(-)$
Re	Reynolds number	$(-)$
S	Suppression factor	$(-)$
T	Temperature	$(℃)$
u	Vector	$(-)$
U	Overall heat transfer coefficient	$(W/m\text{^}2\,℃)$
x	Quality	$(-)$
α	Heat transfer coefficient	$(W/m\text{^}2\,℃)$
$\bar{\alpha}$	Average heat transfer	$(W/m\text{^}2\,℃)$
Δ	Change	$(-)$
ε	Heat exchanger effectiveness	$(-)$

Subscript

$1 \ldots 21$	Coefficients
ch	Charge
ci	At condenser inlet
ei	At evaporator inlet
eli	Input vector to element-wise solver
elo	Output vector to element-wise solver

ext	External fluid
hx	Heat exchanger
i	Input/ inside
ini	Initial
l	Liquid
nb	Nucleate boiling
o	Output/ outside
r	Refrigerant
re	Residual
ri	Refrigerant at inlet
ro	Refrigerant at outlet
s	Secondary fluid
si	Secondary fluid at inlet
so	Secondary fluid at outlet
w	Wall

REFERENCES

Ahilan, C., Kumanan, S., & Sivakumaran, N. (2011a). Online performance assessment of heat exchanger using artificial neural networks. *International Journal of Energy and Environment (IJEE)*, *2*, 829–844.

Ahilan, C., Kumanan, S., & Sivakumaran, N. (2011b). Prediction of Shell and Tube Heat Exchanger Performance using Artificial Neural Networks. *Proc. of the International Conference on Advanced Computing and Communication Technologies (ACCT 2011)*, 307–312.

Chen, J. C. (1966). Correlation for Boiling Heat Transfer to Saturated Fluids in Convective Flow. *Industrial & Engineering Chemistry Process Design and Development*, *5*(3), 322–329. https://doi.org/10.1021/i260019a023

Churchill, S. W., & Bernstein, M. (1977). A Correlating Equation for Forced Convection From Gases and Liquids to a Circular Cylinder in Crossflow. *Journal of Heat Transfer*, *99*(2), 300–306. https://doi.org/10.1115/1.3450685

El-Said, E. M. S., Abd Elaziz, M., & Elsheikh, A. H. (2021). Machine learning algorithms for improving the prediction of air injection effect on the thermohydraulic performance of shell and tube heat exchanger. *Applied Thermal Engineering*, *185*, 116471. https://doi.org/10.1016/j.applthermaleng.2020.116471

Gang, W., & Wang, J. (2013). Predictive ANN models of ground heat exchanger for the control of hybrid ground source heat pump systems. *Applied Energy*, *112*, 1146–1153. https://doi.org/10.1016/j.apenergy.2012.12.031

Gnielinski, V. (1975). New equations for heat and mass transfer in the turbulent flow in pipes and channels. *NASA STI/Recon Technical Report A*, *75*, 8–16.

Hojjat, M. (2020). Nanofluids as coolant in a shell and tube heat exchanger: ANN modeling and multi-objective optimization. *Applied Mathematics and Computation*, *365*, 124710. https://doi.org/10.1016/j.amc.2019.124710

Hwang, T. H., & Yao, S. C. (1986). Forced convective boiling in horizontal tube bundles. *International Journal of Heat and Mass Transfer*, *29*(5), 785–795. https://doi.org/10.1016/0017-9310(86)90130-4

Iyengar, A. S. (2015). Thermal analysis of shell and tube heat exchangers using artificial neural networks. *Ethiopian Journal of Science and Technology*, *8*(2), 107–120. https://doi.org/10.4314/ejst.v8i2.5

Jasim, H. H. (2013). Estimated Outlet Temperatures in Shell-and-Tube Heat Exchanger Using Artificial Neural Network Approach Based on Practical Data. *Al-Khwarizmi Engineering Journal*, *9*(2), 2–20.

Mandavgane, S. A., & Pandharipande, S. L. (2006). Application of ANN for modeling of heat exchanger with concentration as variable. *IJCT Vol.13(2) [March 2006]*. http://nopr.niscair.res.in/handle/123456789/7004

Mohanraj, M., Jayaraj, S., & Muraleedharan, C. (2015). Applications of artificial neural networks for thermal analysis of heat exchangers – A review. *International Journal of Thermal Sciences*, *90*, 150–172. https://doi.org/10.1016/j.ijthermalsci.2014.11.030

Navvab Kashani, M., Aminian, J., Shahhosseini, S., & Farrokhi, M. (2012). Dynamic crude oil fouling prediction in industrial preheaters using optimized ANN based moving window technique. *Chemical Engineering Research and Design*, *90*(7), 938–949. https://doi.org/10.1016/j.cherd.2011.10.013

Pandharipande, S. L., Siddiqui, M. A., Dubey, A., & Mandavgane, S. A. (2004). Optimising ANN architecture for shell and tube heat exchanger modelling. *IJCT Vol.11(6) [November 2004]*. http://nopr.niscair.res.in/handle/123456789/9550

Wang, Q., Xie, G., Zeng, M., & Luo, L. (2006). Prediction of heat transfer rates for shell-and-tube heat exchangers by artificial neural networks approach. *Journal of Thermal Science*, *15*(3), 257–262. https://doi.org/10.1007/s11630-006-0257-6

Wijayasekara, D., Manic, M., Sabharwall, P., & Utgikar, V. (2011). Optimal artificial neural network architecture selection for performance prediction of compact heat exchanger with the EBaLM-OTR technique. *Nuclear Engineering and Design*, *241*(7), 2549–2557. https://doi.org/10.1016/j.nucengdes.2011.04.045

Xie, G. N., Wang, Q. W., Zeng, M., & Luo, L. Q. (2007). Heat transfer analysis for shell-and-tube heat exchangers with experimental data by artificial neural networks approach. *Applied Thermal Engineering*, *27*(5), 1096–1104. https://doi.org/10.1016/j.applthermaleng.2006.07.036

Yin, C., Rosendahl, L., & Luo, Z. (2003). Methods to improve prediction performance of ANN models. *Simulation Modelling Practice and Theory*, *11*(3), 211–222. https://doi.org/10.1016/S1569-190X(03)00044-3

ACKNOWLEDGEMENT

This work was supported by Emerson Commercial and Residential Solutions. The views and opinions portrayed in this paper are that of the authors only.